Mössbauer study of stage-2 $FeCl_3$-graphite

M. Prietsch, G. Wortmann, and G. Kaindl
Institut für Atom- und Festkörperphysik, Freie Universität Berlin, D-1000 Berlin 33, Germany

R. Schlögl
Institut für Physik, Universität Basel, CH-4056 Basel, Switzerland

(Received 9 August 1985)

^{57}Fe Mössbauer spectroscopy was employed to investigate electronic charge transfer as well as the local structural and magnetic properties of stage-2 $FeCl_3$-graphite in the temperature range from 1.5 to 300 K. Both Fe^{3+} and Fe^{2+} ions were clearly identified in the intercalant layers. The highly textured absorbers, with the graphite c axis preferentially normal to the absorber plane, were investigated in different orientations with respect to the γ rays. In this way, the relative amount of Fe^{2+} ions could be determined over the whole temperature range as 19%, independent of temperature, in disagreement with previous reports. The relaxationlike Mössbauer spectra observed at temperatures between 40 and 100 K reveal a thermally induced electron hopping between Fe^{2+} and Fe^{3+} sites, with an activation energy of 45 ± 20 meV. In addition, the Debye-Waller factor was found to be anisotropic as a consequence of a larger in-plane Fe vibrational amplitude. The magnetically split Mössbauer spectra at temperatures below 4.2 K, which were also studied in external magnetic fields, favor a spin-glass type of magnetic ordering of the intercalant layers.

I. INTRODUCTION

Graphite intercalation compounds (GIC's) are widely investigated because of their quasi-two-dimensional structure and related properties. Of particular interest are their highly anisotropic electrical transport and magnetic properties.[1] Within the group of magnetic GIC's, $FeCl_3$-graphite has attracted considerable attention, and so its preparation conditions and structural properties are well known.[1-8] An interesting aspect of this compound lies in the fact that anhydrous $FeCl_3$ itself is already characterized by a layered structure, which is retained upon intercalation: $FeCl_3$-graphite therefore represents a multilayered intercalant incommensurate with the graphite host [see Fig. 1(a)]. It may be described as a weak acceptor GIC, since the Fermi level of pristine graphite is lowered by only $\simeq 0.7$ eV upon intercalation of $FeCl_3$, as previously concluded from x-ray photoemission spectroscopy and electron-energy-loss spectroscopy results.[7,8]

According to this weak electronic charge transfer from the graphite host to the intercalant, most of the Fe ions remain in the trivalent state. Only around 20% of the intercalated Fe atoms were found, at least at low temperatures, in the divalent state, corresponding to a charge transfer of about 0.2 electrons per intercalated $FeCl_3$ molecule. This behavior is clearly reflected in the ^{57}Fe Mössbauer spectra of various $FeCl_3$-graphite samples taken at temperatures around 10 K, where the Fe^{3+} and Fe^{2+} sites can be easily distinguished by their different spectral parameters.[2,3,9,10] At higher temperatures, however, the Fe^{2+} site cannot be separated readily in the Mössbauer spectra. Several explanations were presented for this peculiar temperature behavior, ranging from a temperature-dependent charge transfer to thermally activated electron hopping processes. Recently, a detailed

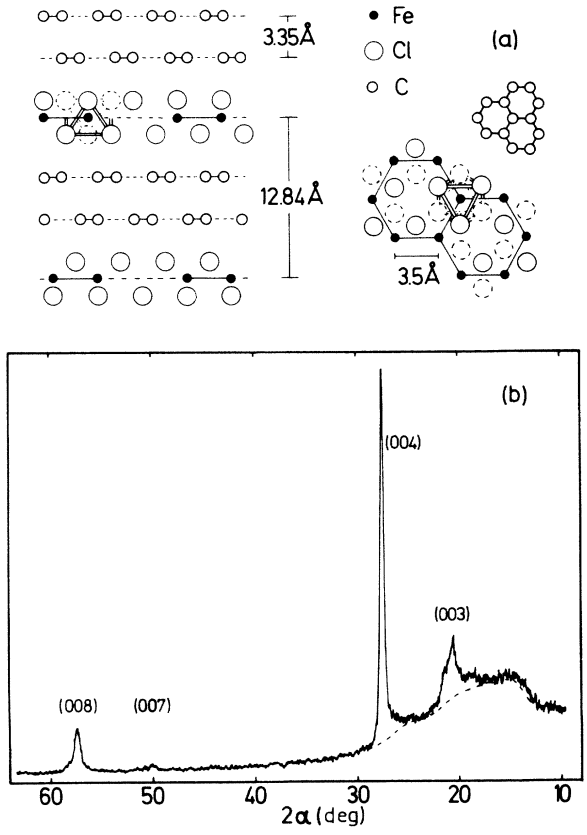

FIG. 1. Structure of $FeCl_3$-graphite. (a) shows the structural model of stage-2 $FeCl_3$-graphite (left: orthogonal to c, right: parallel to c). (b) shows the x-ray diffraction pattern [(00l) reflexes] of a highly textured sample of $FeCl_3$-graphite, obtained using Cu K_α radiation. The dashed line represents the background produced by the Kapton foil used to support the sample.

analysis of Mössbauer spectra of a stage-2 $FeCl_3$-graphite sample led to the assumption of a strong temperature dependence of the electronic charge transfer in this compound.[10]

The magnetic properties of stage-2 $FeCl_3$-graphite are still the subject of controversial discussions. Magnetic susceptibility measurements exhibit field-dependent maxima in the susceptibility, from which two ordering temperatures around 1.7 K were derived, with a generally in-plane antiferromagnetic structure.[11,12] Previous Mössbauer investigations revealed magnetically split hyperfine spectra below 4 K,[2] with a temperature-dependent line broadening which was assumed to be caused by magnetic relaxation processes. The Mössbauer results were interpreted with different models, favoring either superparamagnetism[4] or an antiferromagnetic in-plane spin arrangement.[3] The existence of a well-defined antiferromagnetic structure in stage-2 $FeCl_3$-graphite, however, was recently questioned in two different investigations: A neutron-diffraction study gave no evidence for long-range order of the Fe spins,[13] and, furthermore, a spin-glass state of the iron spins was proposed in a combined Mössbauer and susceptibility study.[14]

In the present paper, we report on an ^{57}Fe Mössbauer study of a stage-2 $FeCl_3$-graphite sample, which was produced from natural graphite flakes by a novel intercalation technique.[15] Highly textured absorbers were investigated with the γ rays at different angles with respect to the graphite c axis. This allowed us to monitor the Fe^{2+} species, which is otherwise masked by fast relaxation processes above 100 K, over the whole temperature range from 1.5 to 300 K. The relative amount of Fe^{2+} ions was found to be temperature independent. The electron-hopping rates between Fe^{2+} and Fe^{3+} were found to follow an Arrhenius behavior with an activation energy of 45 ± 20 meV. Employing highly textured absorbers, we were able to observe the anisotropy of the Debye-Waller factor. In addition to this, the magnetic properties of stage-2 $FeCl_3$-graphite were investigated in the temperature range from 1.5 to 4.2 K, partly in presence of external magnetic fields. The results favor the formation of a spin-glass state within the intercalated layers, while there is no evidence for superparamagnetism.

II. EXPERIMENTAL

Natural graphite flakes from Kropfmühl (Bavaria) with diameters around 1 mm (type S40) were used for the intercalation. Due to the relatively low defect concentration, natural graphite can be intercalated more homogeneously than synthetic highly oriented pyrolytic graphite samples, which were employed in most of the previous studies of $FeCl_3$-graphite. The intercalation was carried out in a solution of $FeCl_3$ in CCl_4 under irradiation of soft uv light.[15] In comparison to the usual vapor phase reaction, which takes place in the presence of $FeCl_3$ and Cl_2 vapor,[7] this method avoids the incorporation of large amounts of excess chlorine. As shown previously,[5] the typical Cl:Fe ratio of vapor phase doped $FeCl_3$-graphite from S40 material is 3.04, while a chemical analysis of the present sample yielded 3.01. This results in a more homogeneous intercalation. In particular, the formation of Fe vacancies in the $FeCl_3$ sublattice is strongly reduced. An x-ray diffraction analysis of the highly textured sample showed only (00l) reflections, originating from stage-2 $FeCl_3$-graphite with a c-axis periodicity of 12.84 ± 0.03 Å [see Fig. 1(b)]. No evidence for the presence of unintercalated graphite was found. A slight broadening of the (003) and (007) reflections, as well as the absence of (005) and (006) reflections, indicated staging defects in the sample, with a staging uncertainty of $\simeq0.2$. This means that the stage of the studied sample can be given as 2.0 ± 0.2.

$FeCl_3$-graphite, like anhydrous $FeCl_3$, is highly hygroscopic.[5,6] The sample was therefore handled in a purified argon atmosphere. When the absorbers were prepared, the flakes oriented themselves parallel to the absorber plane, resulting in highly textured absorbers with the graphite c axis perpendicular to the absorber plane. The Mössbauer measurements were performed with the c axis parallel to the γ-ray direction ($\alpha=0°$) or tilted by the so-called magic angle ($\alpha=54.7°$); measurements were also performed in an external magnetic field which was applied parallel to the γ-ray direction, with the absorber tilted by $\alpha=72°$ (see Table I). The temperature of the absorber was determined using either a Ge diode, a Pt resistor, or the vapor pressure of the liquid-He bath. In the range from 1.5 to 10 K, the temperature varied during the measurements by less

TABLE I. Summary of studied Mössbauer absorbers of stage-2 $FeCl_3$-graphite (samples 1–4) and of anhydrous $FeCl_3$ (sample 5), including details of the experimental conditions: d is the absorber thickness, T_S and T_A are the respective temperatures of the source and the absorber, and α is the angle between the γ-ray direction and the normal to the absorber plane.

Sample	d (mg/cm^2)	T_S (K)	T_A (K)	α (deg)	B_{ext} (T)	Capsule
1	56	300	1.6–300	0	0	Al with Be windows
2	13	He	10.6	0, 54.7	0	Plastic
3	17	300	300	0, 54.7	0	Plastic
4	15	He	1.5–4.2	72	0–5	Kapton tape
5	40	300	1.5–300	(Powder)	0	Al with Be windows

than 0.1 K, and at higher temperatures it varied by less than 0.3 K. The Mössbauer measurements were performed in standard transmission geometry with a sinusoidally moved source; the velocity was calibrated using the magnetic splitting of natural iron metal. The isomer shift of the employed $^{57}CoRh$ source relative to metallic iron was found to be 0.105 mm/s. In order to make a comparison, the respective temperature dependences of isomer shift, Debye-Waller factor and magnetic hyperfine splitting were also investigated for anhydrous $FeCl_3$.

III. ELECTRON HOPPING AND CHARGE TRANSFER

The electron-hopping process and the electronic charge transfer of stage-2 $FeCl_3$-graphite can be studied in a straightforward way by Mössbauer spectroscopy at temperatures above 10 K, where line broadenings and spectral splittings due to magnetic hyperfine interactions are absent. This is clearly seen in the spectra in Fig. 2, which were recorded with $\alpha=0°$ at temperatures between 10 and 300 K. At low temperatures a main absorption line due to Fe^{3+} ions and a satellite line originating from Fe^{2+} ions is observed. The latter is part of a quadrupole doublet, with the other component hidden under the Fe^{3+} component [see also Fig. 3(a)]. With increasing temperatures, the Fe^{2+} satellite line broadens, becomes asymmetric, and is finally no longer visible in the spectra.

In agreement with other authors,[3,10] we assume that an electronic relaxation process originating from thermally activated electron hopping between Fe^{2+} and Fe^{3+} ions is responsible for the observed spectral behavior. Above 100 K the relaxation rate is so high that the different valence

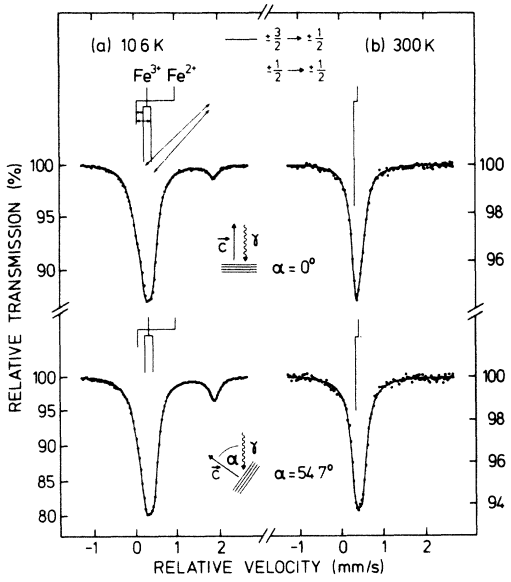

FIG. 3. ^{57}Fe Mössbauer spectra of highly textured $FeCl_3$-graphite absorbers at two different orientations and temperatures. (a) shows the spectra at 10.6 K (sample 2). The relaxation model is schematically given on top: The solid and dotted vertical bars correspond to different nuclear transitions; the arrows symbolize the two-level systems (see the text). (b) shows the spectra at 300 K (sample 3). In the limit of fast relaxation, each spectrum consists of two lines according to the two nuclear transitions. The intensity ratio is the same as for the Fe^{2+} site at 10.6 K. Note that the resonance absorption effect at 300 K changes only slightly upon tilting of the absorber, despite an increase of the effective absorber thickness by the geometrical factor of $\sqrt{3}$.

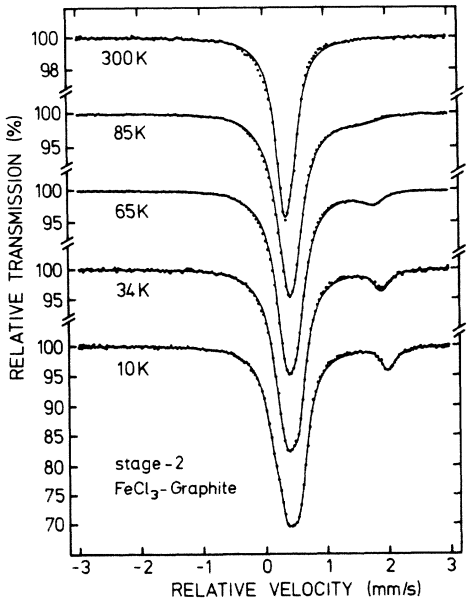

FIG. 2. Representative ^{57}Fe Mössbauer spectra of stage-2 $FeCl_3$-graphite (sample 1) at $\alpha=0°$ and at temperatures in the range from 10 to 300 K. The solid lines through the data points represent the results of least-squares fits (see the text).

states are no longer resolved. Electron hopping has been investigated previously by Mössbauer spectroscopy for various other compounds, such as Eu_3S_4 (Ref. 16) and FeOCl (Ref. 17). In those cases the relaxation-modulated resonance spectra were fitted by corresponding relaxation models yielding rate and activation energy of the electron-hopping processes involved. In order to investigate electron hopping in $FeCl_3$-graphite, we first discuss the spectra obtained at low temperatures because the relaxation is slow enough in this region to provide a static picture of the Fe^{3+} and Fe^{2+} ions.

A. Static limit

Mössbauer spectra of $FeCl_3$-graphite (sample 2) at 10.6 K are given in Fig. 3(a) for two geometries. They clearly show the presence of a majority Fe^{3+} site with a small quadrupole interaction $[\Delta E_Q(3+)=0.18$ mm/s] and a minority Fe^{2+} site with a large quadrupole interaction $[\Delta E_Q(2+)=-1.86$ mm/s]. The quadrupole doublets of the two sites exhibit different dependences of their ratios of line intensity on geometry: For the Fe^{3+} site it is close to 1:1 in both orientations, while for the Fe^{2+} site, the intensity ratio is 2.6:1 at $\alpha=0°$, and 1:1, as expected, at

$\alpha=54.7°$. At the so-called magic angle, $\alpha=54.7°$, the quadrupole doublets of textured absorbers generally exhibit a 1:1 intensity ratio. The observed orientation dependence proves that the main axis of the electric field gradient (EFG) at the Fe^{2+} sites is directed parallel to the c axis. The slight deviation from the ratio of 3:1 expected for $\alpha=0°$ is caused by an incomplete texture of the studied absorber resulting in a distribution of c axes with a mean deviation of $\Delta\alpha\simeq 16°$. This is also confirmed by the spectra taken in the magnetically ordered state (see below).

The origins of the electric quadrupole interactions at the two Fe sites as well as their different behavior upon tilting of the absorber will be discussed below. We will first describe the employed relaxation model, where we assume that the axes and signs of the EFG at the Fe^{3+} sites are randomly distributed.

B. Relaxation model

Based on the static spectra observed at 10.6 K, the relaxation spectra contain four components [see Fig. 3(a)]. Due to electron hopping between Fe^{2+} and Fe^{3+} sites, transitions between all four components of the two quadrupole doublets are possible. In addition, mixing of the two nuclear transitions may occur because of the different quantization axes (the main axes of the EFG) of the Fe^{2+} and Fe^{3+} states. Such a four-level system is difficult to handle; on the other hand, an analytical solution exists for the line shape of a two-level system:[18,19]

$$I(\omega)=\mathrm{Im}\left[\frac{r(2)(\omega-\omega_1+i\Gamma_1)+r(1)(\omega-\omega_2+i\Gamma_2)+i(p_{1\to 2}+p_{2\to 1})}{(\omega-\omega_1+i\Gamma_1+ip_{1\to 2})(\omega-\omega_2+i\Gamma_2+ip_{2\to 1})+p_{1\to 2}p_{2\to 1}}\right]. \tag{1}$$

Here ω_j is the line position, Γ_j the half linewidth, $r(j)$ the relative intensity, and $p_{j\to k}$ the probability for a transition from j to k. Thus, the condition of balance $r(1)p_{1\to 2}=r(2)p_{2\to 1}$, with $r(1)+r(2)=1$, must be fulfilled. In the present case, we may describe the four-level system in good approximation by a superposition of several two-level systems, since the electric quadrupole interaction at the Fe^{3+} site is so small.

At 10.6 K the electric quadrupole splitting at the Fe^{2+} site is by a factor of 10 larger than that at the Fe^{3+} site. We may therefore neglect the Fe^{3+} electric quadrupole splitting in a first approximation. This means that the nuclear quantization direction at the Fe^{2+} site, which is parallel to c, may also be kept for the Fe^{3+} site. The relaxation spectrum consists of two subsystems, given by the $\pm\frac{3}{2}\to\pm\frac{1}{2}$ and the $\pm\frac{1}{2}\to\pm\frac{1}{2}$ nuclear transitions in the Fe^{2+} state. No mixing between these two subsystems will take place in the Fe^{3+} state; this means that the nuclear quantum numbers are well-defined during the electron-hopping process. We can thus describe the spectrum as a sum of two independently relaxing two-level systems. The intensity ratio of the contributions of the two nuclear transitions to the Fe^{3+} line is the same as the polarization-dependent intensity ratio of the Fe^{2+} quadrupole doublet. This simplified relaxation model satisfactorily describes the situation in the limit of fast relaxation at temperatures above 100 K. In the region below $\simeq$100 K, however, the electric quadrupole interaction at the Fe^{3+} site must also be taken into account.

For $\Delta E_Q(3+)\ll-\Delta E_Q(2+)$, the system may be described by four two-level systems as indicated by the arrows in Fig. 3(a). We have to assume that both Fe^{3+} levels contribute with equal intensity to the Fe^{2+} nuclear transitions [shown by the solid and dotted bars in the diagram of Fig. 3(a)]. Since the quantization axes of the Fe^{2+} and Fe^{3+} states are not parallel, a slow mixing of the four subsystems will occur, with a rate equal to the Fe^{3+} quadrupole splitting. Since sign and quantization direction of the Fe^{3+} EFG are unknown, this mixing cannot be accounted for in a quantitative way in the present relaxation model. However, by comparing the relative magnitudes of $\Delta E_Q(3+)$ and of the linewidth W with the relaxation rates $p_{2+\to 3+}$ and $p_{3+\to 2+}$, it can be shown that this mixing gets only important in the intermediate range of relaxation rates, where $p_{2+\to 3+}>W$, and $p_{3+\to 2+}<\Delta E_Q(3+)$ hold.

For slow relaxation, with hopping frequencies smaller or close to the linewidth ($p_{2+\to 3+}<W$), at most one hopping event will happen in the time window defined by the natural width. Hence, transitions between more than two levels can be neglected because of their negligible effects on lineshape, and no mixing has to be taken into account. For relaxation which is fast compared to the Fe^{3+} electric quadrupole splitting [$p_{3+\to 2+}>\Delta E_Q(3+)$], only a very small amount of mixing will occur, since the time spent in the Fe^{3+} state is too short for a change of the quantization direction. The next relaxation event back to the Fe^{2+} state will reinforce the Fe^{2+} nuclear quantum number due to the large Fe^{2+} electric quadrupole splitting. The Fe^{2+} quantization axis determines the spectrum at fast hopping rates. In the Fe^{3+} state, the effective electric quadrupole splitting vanishes at fast hopping rates, because the nucleus feels only the average of the two energy levels during the short time intervals it remains in the Fe^{3+} state (motional narrowing); this does not mean, however, that the EFG at the Fe^{3+} site actually vanishes.

In the limit of fast relaxation the spectrum consists of two absorption lines with relative intensities as given by the orientation of the EFG at the Fe^{2+} site. Such spectra have been reported before (see for example Fig. 5b in Ref. 5), but they were interpreted as being due to two Fe^{3+} sites with different isomer shifts and unequal relative intensities. According to the lever rule, the line positions in the present model are given by

$$L_1=r(3+)S(3+)+r(2+)[S(2+)+\tfrac{1}{2}\Delta E_Q(2+)], \tag{2a}$$

$$L_2=r(3+)S(3+)+r(2+)[S(2+)-\tfrac{1}{2}\Delta E_Q(2+)]. \tag{2b}$$

TABLE II. Results from least-squares fits of the Mössbauer spectra of stage-2 $FeCl_3$-graphite in the temperature range from 10 to 300 K. T_A is the absorber temperature, α the tilt angle, S the isomer shift, W the line width (full width at half maximum), ΔE_Q the electric quadrupole splitting, I the intensity ratio of the quadrupole doublet [$I(3+)=1:1$ for all measurements], t the reduced absorber thickness (Ref. 20), and $p_{2+\to 3+}$ the electron-hopping rate. Typical errors are $\Delta S=0.01$ mm/s, $\Delta(\Delta E_Q)=0.02$ mm/s, $\Delta W=0.02$ mm/s, $\Delta I=0.1$, $\delta t=0.01$, and $\delta p_{2+\to 3+}=0.2$. An asterix denotes that this parameter was kept constant during the fit.

Sample	T_A (K)	α (deg)	$S(3+)$ (mm/s)	$S(2+)$ (mm/s)	$W(3+)$ (mm/s)	$W(2+)$ (mm/s)	$\Delta E_Q(3+)$ (mm/s)	$\Delta E_Q(2+)$ (mm/s)	$I(2+)$	t	$p_{2+\to 3+}$ (mm/s)
1	10	0	0.45	1.08	0.29	0.28	0.19	−1.86	2.6:1	3.98	0.00*
1	34	0	0.44	1.08	0.28	0.28*	0.17	−1.67	2.6:1*	3.68	0.02
1	65	0	0.44	1.07	0.32	0.28*	0.18	−1.46	2.6:1*	3.24	0.10
1	85	0	0.43	1.06	0.34	0.28*	0.14	−1.32	2.6:1*	2.95	0.25
1	180	0	0.37	1.01	0.34	0.28*	0.07	−1.05	2.6:1*	1.70	9
1	300	0	0.30	0.94	0.33	0.28*	0.00	−0.78	2.6:1*	0.83	→ ∞
2	10.6	0	0.31	0.95	0.31	0.30	0.17	−1.87	2.6:1	0.94	0.00*
2	10.6	54.7	0.32	0.95	0.29	0.30	0.18	−1.87	1:1*	1.56	0.00*
3	300	0	0.30	0.94	0.28	0.28*	0.00	−0.81	2.8:1	0.294	→ ∞
3	300	54.7	0.30	0.94	0.28	0.28	0.00	−0.81	1:1*	0.392	→ ∞

The observed quadrupole splitting ΔL and the averaged isomer shift $\bar{S}$ are then given by

$$\Delta L = L_2 - L_1 = -\Delta E_Q(2+) r(2+) , \tag{3a}$$

$$\bar{S} = r(3+) S(3+) + r(2+) S(2+) . \tag{3b}$$

The described relaxation model is confirmed well by the results of our measurements with different orientations of the absorber [see Fig. 3(b) and Table II]. The two absorption lines observed at 300 K (at $L_1=0.35$ mm/s and $L_2=0.50$ mm/s) show an intensity ratio of 2.8:1 at $\alpha=0°$ and 1:1 at $\alpha=54.7°$. This corresponds to $\Delta L=0.15$ mm/s and $\bar{S}=0.42$ mm/s.

C. Least-squares-fit results and discussion

The relaxation model described above yields excellent least-squares fits of the measured spectral shapes in the temperature range from 1 .o 300 K (see Fig. 2). This holds even for the spectra taken around 90 K, where the relaxation rates are in the intermediate range between slow and fast relaxation, that is, where $p_{2+\to 3+}$ ($\simeq 0.40$ mm/s) is larger than the linewidth ($\simeq 0.30$ mm/s) and $p_{3+\to 2+}$ ($\simeq 0.09$ mm/s) is smaller than $\Delta E_Q(3+)$ ($\simeq 0.15$ mm/s). In this region mixing effects could lead to deviations of the relaxation-model line shapes from the actual spectra. Appreciable deviations, however, are not observed, possibly due to the narrowness of the temperature range where intermediate relaxation rates actually occur.

Because of absorber thickness effects, the spectra were fitted with line shapes obtained by the transmission integral.[20] This was found to be essential in order to extract reliable values for $r(2+)$, especially at temperatures below 80 K. Without the use of the transmission integral, a larger Fe^{2+} content [$r(2+)\simeq 25\%$] was obtained from the spectra measured at temperatures below 80 K. This would simulate a temperature-dependent charge transfer, since at higher temperatures a smaller Fe^{2+} content [$r(2+)\simeq 19\%$] is obtained. We would like to stress here that in earlier Mössbauer work, where $r(2+)\simeq 25\%$ was reported, fits without the use of the transmission integral were carried out.[9,21] Such a comparatively large $r(2+)$ value at low temperatures led to an Fe^{2+} superlattice model,[9] which now becomes very doubtful in view of our results.

At fast relaxation rates, strong correlations between $S(2+)$, $S(3+)$, $\Delta E_Q(2+)$, and $r(2+)$ [see Eqs. (2a) and (2b)] are expected. In order to extract reliable results for $\Delta E_Q(2+)$ and $r(2+)$ from the spectra recorded above 80 K, we assumed the temperature variation of $S(3+)$, caused by the second-order Doppler effect, to have the same slope as for anhydrous $FeCl_3$ [see Fig. 4(a)]. In addition, the difference $S(2+)-S(3+)$ was kept constant at a value of 0.64 mm/s, as obtained at 10.6 K, and the intensity ratio of the Fe^{2+} doublet was set equal to 2.6:1 for all temperatures studied.

As a result of these fits, we obtain the fraction of the Fe^{2+} ions in the intercalant, $r(2+)=(19\pm 2)\%$, independent of temperature. This means that there is no temperature-induced charge transfer from the graphite host to $FeCl_3$, which would lead to a variation of $r(2+)$.

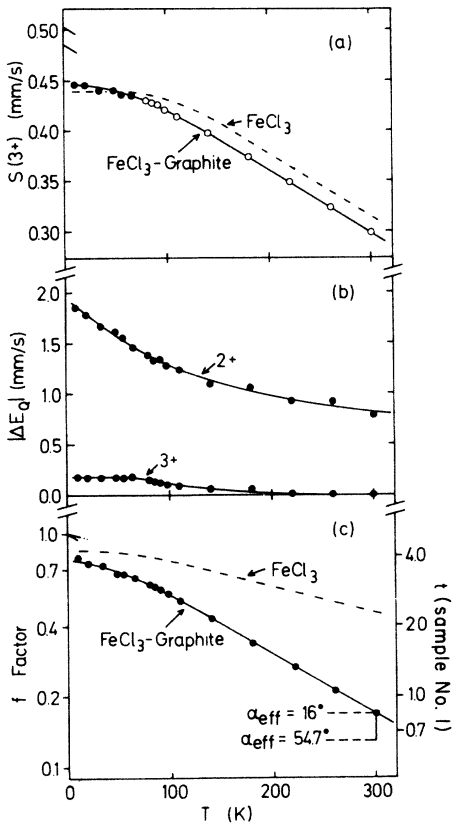

FIG. 4. (a) Isomer shift of the Fe^{3+} site in comparison to anhydrous $FeCl_3$. Solid circles represent experimental values; open circles represent adopted values, assuming the same temperature variation of the isomer shift as for anhydrous $FeCl_3$. (b) Temperature dependence of the magnitude of the electric quadrupole splitting, $|\Delta E_Q|$, of the Fe^{2+} and the Fe^{3+} sites. (c) Temperature dependence of the f factor obtained from the reduced absorber thickness t. For the tilted absorber, the real area is reduced by the geometrical factor of $\sqrt{3}$.

Our present result for $r(2+)$ corresponds to a charge transfer of about 0.015 electrons per carbon atom, if the typical sum formula for stage-2 $FeCl_3$-graphite, $C_{13}FeCl_3$, is assumed.

The electric quadrupole splitting at the Fe^{2+} site, $\Delta E_Q(2+)$, varies with temperature from -1.86 mm/s at 10 K to -0.81 mm/s at 300 K [see Fig. 4(b)]. Up to $\simeq$80 K, $\Delta E_Q(2+)$ is obtained directly from the position of the satellite line. Above that temperature, $\Delta E_Q(2+)$ must be derived indirectly from the relaxation-model fits of the spectra. At 300 K, $\Delta E_Q(2+)$ was extracted from the measurements with different transmission geometries [see Fig. 3(b)] according to Eq. (3a). The observed temperature dependence of $\Delta E_Q(2+)$ [see Fig. 4(b)] is typical for ferrous Fe and arises from the temperature-dependent occupation of the $3d$ ligand orbitals.[22] The direction of the EFG axis at the Fe^{2+} sites is most probably connected with a distortion of the nearest-neighbor octahedron of chlorine atoms due to interaction with the graphite planes, giving rise to a threefold symmetry axis parallel to c. It is reasonable to assume that the Fe^{2+} ions have no Fe^{2+} nearest neighbors, since a strong repulsion of neighboring Fe^{2+} ions would be expected because they would act as negatively charged defects in the intercalant lattice.

The obtained fit results for the electric quadrupole splitting of the Fe^{3+} site [see Fig. 4(b)] are strongly correlated with the Fe^{3+} linewidth; thus variations of both parameters may actually occur. $\Delta E_Q(3+)$ vanishes above $\simeq$150 K due to motional narrowing as described above. The origin of the electric quadrupole interaction at the Fe^{3+} site is not obvious. In this respect we note that an electric quadrupole interaction is not resolved in the Mössbauer spectra of anhydrous $FeCl_3$; this gives support to our view that the EFG at the ferric site in $FeCl_3$-graphite is caused by a distorted nearest-neighbor coordination shell of Cl ions.

Several reasons for the absence of a dependence of the intensity ratio of the Fe^{3+} quadrupole doublet on the orientation of a textured absorber have been discussed.[10] We propose the following explanation for this observation: The EFG is caused by two components, a contribution due to chlorine neighbors with the main axis parallel to c, and a contribution due to Fe^{2+} neighbors with the axis perpendicular to c. Therefore, the resulting EFG tensor will not be axially symmetric, and its main axis is expected to point in a direction close to the magic angle relative to c. This would mean that both the asymmetry and the orientation of the EFG tensor prevent an orientation dependence of the intensity ratio of the quadrupole doublet. It should be close to 1:1, independent of the direction of the γ rays with respect to the orientation of the absorber.

The electron-hopping rates are assumed to follow the Arrhenius law:

$$p_{2+\rightarrow 3+} \propto e^{-E_A/k_B T}, \tag{4}$$

where E_A represents the activation energy. In Fig. 5 we

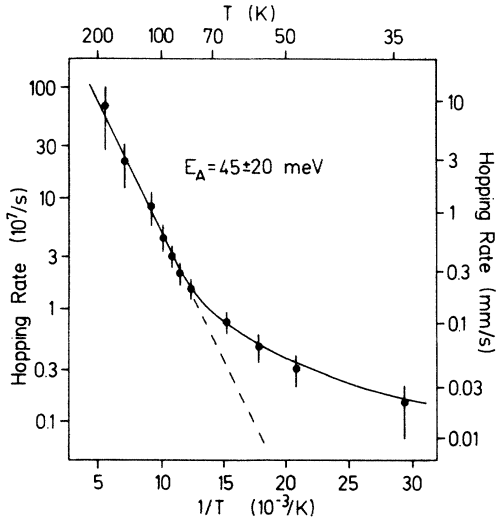

FIG. 5. An Arrhenius plot of the electron-hopping rate $p_{2+\rightarrow 3+}$. The larger error bars at low or high temperatures are due to strong correlations between linewidth and relaxation rate. At low temperatures, tunneling effects contribute to the hopping rate, causing the observed deviation from a linear relationship.

show the rates obtained from the relaxation-model fit in the usual Arrhenius plot. Above 70 K an activation energy of 45 ± 20 meV can be derived from the slope of the linear dependence. Below 70 K electron tunneling events may also contribute to the electron-hopping process: This would readily explain the observed deviation from a linear relationship at low temperatures. Our results for the activation energy E_A agree well with those obtained for a similar quasi-two-dimensional system (FeOCl intercalation compounds), which also contains Fe^{2+} and Fe^{3+} ions involved in charge fluctuations due to electron hopping.[17]

IV. ANISOTROPY OF THE DEBYE-WALLER FACTOR

It is by now well established that Mössbauer spectroscopy can monitor the anisotropy of chemical bonding at intercalated Mössbauer atoms in GIC's by measuring the recoil-free fraction of γ-ray absorption (f factor) in different directions relative to a highly textured absorber.[23–25] The present study of $FeCl_3$-graphite also shows an anisotropy of the f factor. From the temperature dependence of the reduced absorber thickness t, measured parallel to the graphite c axis [see Fig. 4(c)], as well as from measurements with tilted absorbers, we calculate Debye temperatures $\Theta_D^{\parallel}=129$ K (parallel to the graphite planes) and $\Theta_D^{\perp}=146$ K (perpendicular to the graphite planes, see Table III). In this analysis, the angular distribution of the graphite c axes in the studied absorbers (incomplete texture) was taken into account.

The anisotropy in the Debye temperatures and in the related mean-squared vibrational amplitudes (see Table III) shows that the Fe ions are stronger bound in c direction than parallel to the graphite planes: This has also been observed for other GIC's. In $FeCl_3$-graphite the anisotropy is not as strongly pronounced as in several other GIC's, such as Cs-graphite,[23] SbF_5-graphite,[24] and IF_5-graphite.[25] The difference may be related to the relatively homogeneous $FeCl_3$-sandwich structure as well as to the quasioctahedral chlorine surrounding of the Fe ions. The Debye temperatures extracted in the present work were used to derive the zero-point vibrations and thereby also the nonlinear thermal variation of the isomer shift in the low-temperature region [see Fig. 4(a)].

It is important to note that the averaged Debye temperature of the intercalant ($\Theta_D=135$ K) is considerably smaller than that of pure $FeCl_3$ powder ($\Theta_D=220$ K). The latter was derived from the temperature dependence of the f factor of a powdered $FeCl_3$ absorber [see Fig. 4(c)]. As is mentioned above, anhydrous $FeCl_3$ also forms a layered sandwich structure.[26] The lower Debye temperature observed for $FeCl_3$-graphite may be due in part to the incommensurate intercalation of a single $FeCl_3$ layer into the graphite planes and in part to the Fe^{2+} admixture in the intercalant.

V. MAGNETIC HYPERFINE INTERACTIONS

From the results of susceptibility measurements, stage-2 $FeCl_3$-graphite is known to undergo magnetic ordering around 1.7 K.[11,12] Previous Mössbauer studies of stage-2 $FeCl_3$-graphite revealed magnetic-relaxation spectra below 3 K and a static magnetic hyperfine splitting at 65 mK.[2] In the present work, the magnetic behavior of the sample was studied in detail at temperatures between 1.6 and 4.2 K (see Fig. 6).

The spectrum recorded at 4.2 K already shows a broadening of the Fe^{3+} component, i.e., an increase in linewidth, in comparison to the 10-K spectrum of the same absorber. The spectra obtained at 3.0, 2.6, 2.2, and 1.6 K show the successive development of magnetic sextet patterns for the Fe^{3+} site, accompanied by strong line-broadening effects at intermediate temperatures. The observed spectral shapes are typical for magnetic-relaxation spectra.[27] On the other hand, since the broadenings of the six lines are not identical at the onset of magnetic relaxation, a temperature-dependent distribution of hyperfine splittings also contributes to the spectra at 2.2 and 2.6 K. An explanation for the occurrence of these complex magnetic hyperfine spectra will be given below, where the results of measurements taken in external magnetic fields are also presented.

A. Static magnetic hyperfine spectrum

We first turn to the spectrum at 1.6 K, where line-broadening effects are almost absent. It consists of three

TABLE III. Angular dependence of Debye temperatures Θ_D of stage-2 $FeCl_3$-graphite; for comparison, the results for anhydrous $FeCl_3$ are also shown. α (α_{eff}) is the real (effective) tilt angle, where α_{eff} is determined from the intensity ratio of the quadrupole doublet, f is the f factor, and $\langle x^2\rangle$ is the mean-squared vibrational amplitude. Typical errors are $\Delta f=0.01$, $\Delta\langle x^2\rangle=0.001$ Å^2, and $\Delta\Theta_D=3$ K. The values for $\alpha_{\text{eff}}=0°$ and $\alpha_{\text{eff}}=90°$ are calculated from the experimental values for $\alpha=0°$ and $\alpha=54.7°$, respectively.

	α (deg)	α_{eff} (deg)	f (300 K)	$\langle x^2\rangle$ (Å^2)	Θ_D (K)
		0	0.150	0.036	146
$FeCl_3$ graphite	0	16	0.144	0.036	144
	54.7	54.7	0.109	0.042	135
		90	0.098	0.046	129
Anhydrous $FeCl_3$			0.44	0.015	220

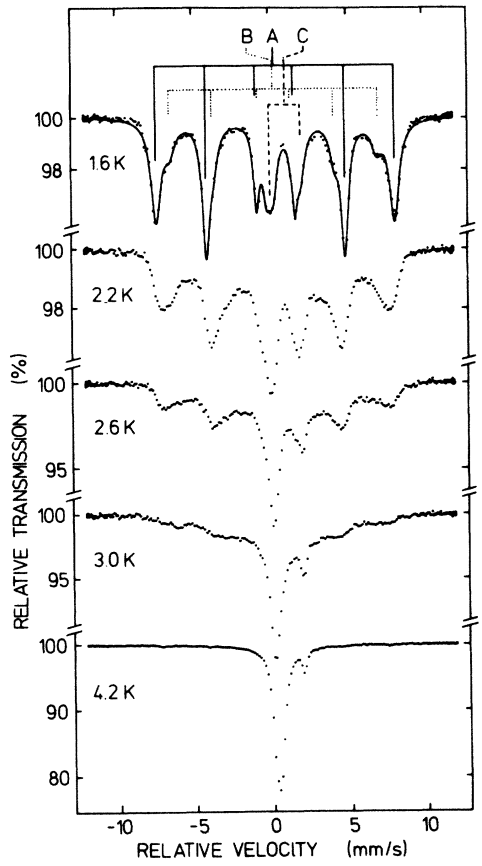

FIG. 6. Representative ^{57}Fe Mössbauer spectra of stage-2 $FeCl_3$-graphite (sample 1) with $\alpha=0°$, in the temperature range from 1.6 to 4.2 K.

subspectra, which are assigned to three different Fe sites, labeled A, B, and C in Fig. 6 and Table IV. From now on, we will describe the intensity ratio $3:q:1:1:q:3$ of the hyperfine sextet by the parameter q. On the basis of the γ-ray angular distributions of the different nuclear $M1$ transitions, q may adopt values from 0 to 4.[22] A is the majority Fe^{3+} site, split by a magnetic hyperfine field of $B_{\rm eff}(A)=-48.6$ T, with $q(A)=3.4$. B is the minority Fe^{3+} site with a smaller magnetic splitting of $B_{\rm eff}(B)=-42.2$ T, with $q(B)=2.8$, a larger linewidth, and a smaller isomer shift. Both Fe^{3+} sites are characterized by a small distribution of $B_{\rm eff}$ ($\Delta B_{\rm eff}\simeq 3\%$). C denotes the Fe^{2+} site, which exhibits the large electric quadrupole splitting, which is only broadened by small (transferred) magnetic hyperfine fields. The spectrum agrees well with that reported in Ref. 2 for stage-2 $FeCl_3$-graphite at 65 mK. We find, however, that the magnetic field at the minority Fe^{3+} site is directed more parallel to the graphite planes than stated in Ref. 2.

The small deviation of the parameter q of site A from the maximum value ($q=4$) is due to the incomplete texture of the absorber. This deviation corresponds to a mean angle $\Delta\alpha\simeq 16°$ of the c-axis distribution with respect to the γ rays, in excellent agreement with the value obtained from the Fe^{2+} quadrupole spectra at 10.6 K (see above). This indicates a full in-plane alignment of the Fe^{3+}(A) magnetic moments, whereas the site-B moments are less well oriented.

In agreement with previous investigations,[2] we attribute the occurence of two Fe^{3+} sites with slightly different hyperfine fields, q parameters, and isomer shifts to magnetically and chemically different environments of the Fe^{3+} ions at low temperatures. The majority Fe^{3+} site A exhibits a magnetic hyperfine field at saturation, which is practically identical with the one observed for anhydrous $FeCl_3$ ($B_{\rm eff}=-49.3$ T, see Table IV). This prompted previous investigators to attribute site A to regular lattice sites in the $FeCl_3$ intercalant islands, while site B was interpreted to be irregular Fe^{3+} sites at the borderline of the intercalant islands or at Fe vacancies.[2] This model demands a very high Fe vacancy concentration or very small intercalant island sizes. From the site-A-to-site-B intensity ratio one can estimate an island diameter of about 60 Å, which is much smaller than was previously observed in electron-microscopy studies ($\simeq$300 A).[5]

There are two major differences in the magnetic properties of $FeCl_3$-graphite and anhydrous $FeCl_3$, which we want to point out. The latter consists of regularly arranged Fe^{3+} ions and possesses a complex magnetic structure with a spiral out-of-plane arrangement of the Fe^{3+} spins.[26] In our $FeCl_3$-graphite sample, the magnetic Fe^{3+} ions are diluted by nonmagnetic Fe^{2+} ions, and the spins of the Fe^{3+}(A) sites lie parallel to the plane, while those of the Fe^{3+}(B) site are less well oriented. The Fe^{2+} sites can be regarded as randomly distributed, but isolated from each other, because of the Coulomb repulsion of the nega-

TABLE IV. Hyperfine parameters for the different Fe sites in stage-2 $FeCl_3$-graphite at 1.6 K. For the sake of comparison, the results for anhydrous $FeCl_3$ at 1.4 K are also given. S is the isomer shift, W the line width (full width at half maximum), ΔE_Q the electric quadrupole splitting, $B_{\rm eff}$ and $\Delta B_{\rm eff}$ the magnetic hyperfine field and its distribution, respectively, q the intensity parameter of the hyperfine sextet ($3:q:1:1:q:3$). Typical errors are $\Delta S=0.03$ mm/s, $\Delta W=0.02$ mm/s, $\Delta(\Delta E_Q)=0.02$ mm/s, $\Delta(B_{\rm eff})=0.1$ T, $\Delta(\Delta B_{\rm eff})=0.1$ T, $\Delta q=0.2$, and $\Delta r=2\%$.

Site	S (mm/s)	W (mm/s)	ΔE_Q (mm/s)	$B_{\rm eff}$ (T)	$\Delta B_{\rm eff}$ (T)	q	r (%)
Fe^{3+}(A)	0.45	0.34	−0.01	−48.6	1.4	3.4	67
Fe^{3+}(B)	0.35	0.47	−0.05	−42.2	1.4	2.8	18
Fe^{2+}	1.09	0.67	−2.00			0.4	19
$FeCl_3$	0.45	0.26	0.01	−49.3	0.2	2.0	100

tively charged Fe^{2+} impurities. This means that $\simeq 57\%$ $[3r(2+)]$ of the Fe ions are Fe^{3+} species neighboring to Fe^{2+} ions, while the rest ($\simeq 24\%$) are Fe^{3+} ions surrounded by Fe^{3+} neighbors only. These values are very close to the relative spectral weights observed for sites A and B. We therefore present an alternative model, assigning both sites A and B to regularly intercalated Fe^{3+} ions, with site A surrounded by two Fe^{3+} and one Fe^{2+} ion, whereas site B is coordinated by three nearest-neighbor Fe^{3+} ions. Hence, the out-of-plane spin orientation of site B may have the same origin as the spiral spin arrangement in anhydrous $FeCl_3$, whereas the in-plane orientation of the site-A spins is induced by Fe^{2+} neighbors.

We should note here again that we did not observe two different Fe^{3+} sites at temperatures above 10 K. Due to the very small difference in isomer shift, the two sites cannot be resolved in the spectra up to 80 K, where the Fe^{3+} subspectrum is broadened by $\Delta E_Q(3+)$. At higher temperatures, they cannot be resolved, because the electron-hopping process leads to a relaxation between the two Fe^{3+} sites, causing motional narrowing. That results in a single Fe^{3+} component in the Mössbauer spectrum. Thus the existence of two different Fe^{3+} sites at very low temperatures will not affect the relaxation model for the electron-hopping process described above.

The Fe^{2+} ions remain in a nonmagnetic state. The electric quadrupole split subspectrum of the ferrous ions is broadened by a small magnetic hyperfine field, which is probably transferred from the Fe^{3+} neighbors, and which is therefore expected to act perpendicular to the axis of the EFG tensor. One should note here that the same values of $r(2+)$ and t are obtained from the 10 K spectrum and from the magnetically split 1.6 K spectrum, despite widely different resonance effects. This indicates that the essential parameter in the transmission-integral fit, that is the effective recoil-free fraction of the source ($f_{\text{eff}}=0.54$, see Ref. 20), was chosen correctly.

B. Effects of external magnetic fields

In order to gain further information on type and strength of the in-plane magnetic order, Mössbauer spectra were taken in external magnetic fields B_{ext} applied in a direction of $\alpha=72°$ relative to the absorber normal, but parallel to the γ-ray direction.

Representative resonance spectra measured at temperatures between 1.5 and 4.2 K, with B_{ext} from 0 to 5 T, are shown in Fig. 7. We first discuss the spectra at 1.5 K. As is clearly seen in Fig. 7, the absorption lines broadened slightly with increasing external field, while the magnetic hyperfine splitting decreases. The intensities of the second and fifth lines of the hyperfine sextet decrease with respect to the other components, indicating an increasing alignment of the Fe^{3+} spins in the direction of B_{ext}. None of the Fe subspectra show increasing magnetic hyperfine splitting, which would be indicative for antiferromagnetic ordering. Thus, if there exists antiferromagnetic ordering in the absence of external magnetic fields, it is destroyed by fields above $\simeq 1$ T. In the 3.0 and 4.2 K spectra a broadening of the resonance structures combined with the development of a hyperfine sextet is

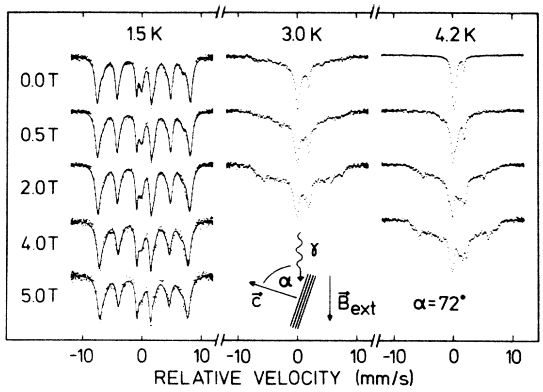

FIG. 7. ^{57}Fe Mössbauer spectra of stage-2 $FeCl_3$-graphite (sample 4), with the absorber tilted by $\alpha=72°$, at 1.5, 3.0, and 4.2 K. The magnitude of the external magnetic field applied parallel to the γ-ray direction is also given.

observed, indicating a field-induced magnetic alignment and/or a decrease of the relaxation rate.

To facilitate the fits of the 1.5-K spectra in the presence of external magnetic fields, the difference $B_{\text{eff}}(\text{A})$-$B_{\text{eff}}(\text{B})$, as well as the relative isomer shifts and electric quadrupole interactions were set to the values found when $B_{\text{ext}}=0$; furthermore, the values of q and the field distributions ΔB_{eff} at sites A and B were set equal.

C. Magnetic interactions in $FeCl_3$-graphite

The effective magnetic hyperfine field at site A, B_{eff}, its distribution, ΔB_{eff}, and the parameter q, resulting from the fits of the 1.5 K spectra, are displayed in Fig. 8 as functions of the magnitude of the external magnetic field. At external fields above 2 T, the magnitude of B_{eff} decreases linearly with a slope of about -0.8; ΔB_{eff} increases with B_{ext} and saturates at about 2 T. The parameter q decreases from $q\simeq 2.0$ at $B_{\text{ext}}=0$ to $q\simeq 1.4$ at $B_{\text{ext}}=5$ T, but a saturation is not observed even at $B_{\text{ext}}=5$ T.

The parameter q observed without external field corresponds to an effective angle of $\alpha_{\text{eff}}=55°$ between the direction of observation (parallel to B_{ext}) and **c**. The difference between α_{eff} and the tilt angle of the absorber plane ($\alpha=72°$) is due to the distribution of the **c** axes of the graphite flakes in the absorber. It should be added here that in this experiment with a large tilt angle, the flakes were held between two layers of Kapton tape; thus, their average angular deviation was larger than in the other measurements, where our standard sample holders were used.

The results of the present measurements in external magnetic fields disagree with the assumption of superparamagnetism in $FeCl_3$-graphite.[4] Superparamagnetic particles, consisting of about 5000 ferromagnetically ordered Fe^{3+} ions (corresponding to islands with diameters of about 300 Å), could be oriented in fields as small as 0.01 T at temperatures below 4.2 K. In this case, we would not observe relaxation spectra for $B_{\text{ext}}\geq 0.5$ T, in

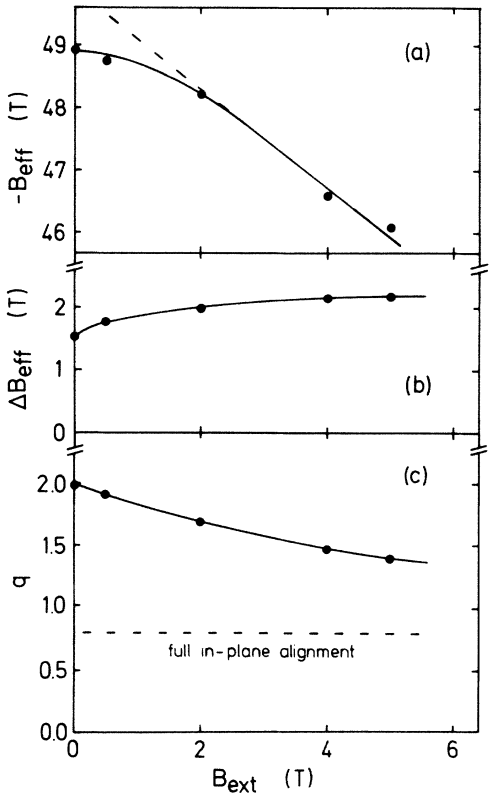

FIG. 8. (a) Effective magnetic hyperfine field, B_{eff}, (b) distribution of hyperfine fields, ΔB_{eff}, and (c) parameter q (from the $3{:}q{:}1{:}1{:}q{:}3$ intensity ratio of the ^{57}Fe hyperfine sextet) at 1.5 K versus applied external magnetic field. The dashed line in (c) corresponds to a full in-plane alignment of the Fe moments.

contrast to our finding (see Fig. 6). In addition, B_{eff} and q would be expected to saturate at very small external fields.

The results presented in Fig. 8 are interpreted in the following way: At $B_{\text{ext}}=0$, the magnetic moments are ordered antiferromagnetically or randomly in-plane. With increasing B_{ext}, the moments become more and more aligned parallel to the in-plane component of B_{ext}. This follows from the gradient of $-B_{\text{eff}}$ versus B_{ext}, which saturates at -0.8, corresponding to an average angle of $\simeq 37°$ between B_{ext} and $-B_{\text{eff}}$, or a tilt angle of about $90°-37°=53°$, in good agreement with $\alpha_{\text{eff}}=55°$. We thus conclude that the external magnetic field is unable to turn the magnetic moments out of the intercalant plane, indicating strong in-plane magnetic interactions of the moments. This is in agreement with the observed change of the parameter q. A full parallel in-plane alignment of the magnetic moments would correspond to $q=0.8$ (with $\alpha_{\text{eff}}=55°$), in agreement with the observation that q decreases with B_{ext}, but does not saturate (at $q=1.4$). On the other hand, from the slope of q versus B_{ext} is is unlikely that the parameter q saturates at $q=0$, which would correspond to a spin alignment parallel to B_{ext}. It should be noted that the saturation of $-B_{\text{eff}}$ takes place at lower values of B_{ext} than that of q. This results from the different angular dependences of $-B_{\text{eff}}$ and q. q depends more critically on α and is thus more sensitive to small deviations from the full in-plane spin alignment than $-B_{\text{eff}}$.

A pure antiferromagnetic ordering of the Fe^{3+} ions is not possible because of the 19% Fe^{2+} ions acting as randomly distributed, nonmagnetic impurities. In agreement with Hohlwein *et al.*[3] and the susceptibility measurements of Millman *et al.*,[11,14] we propose a spin-glass model for the magnetic structure of $FeCl_3$-graphite, with a basically antiferromagnetic arrangement of the Fe^{3+} spins leading to a vanishing net moment. This spin structure is modified to a more parallel in-plane alignment by external fields of about 5 T (at 1.5 K). The observed distribution of relaxation rates in the obtained magnetic spectra at temperatures around 2.5 K is due to different magnetic environments of the Fe^{3+} ions, such as Fe^{2+} ions, island borders, defects, or vacancies.

VI. SUMMARY AND CONCLUSION

The main results of this study of stage-2 $FeCl_3$-graphite concern the electronic charge transfer. From the relative amount of Fe^{2+} ions derived from the Mössbauer spectra in the temperature range from 1.5 to 300 K, a temperature-independent charge transfer of 0.19 electrons per intercalated $FeCl_3$ molecule is derived. Over a wide temperature range, the transferred charge is shared by all Fe ions through a thermally induced electron-hopping process with an activation energy of 45 ± 20 meV. At low temperatures, a charge ordering occurs, giving rise to well-defined magnetic Fe^{3+} and nonmagnetic Fe^{2+} sites within the time window of the Mössbauer measurement. Two essential points of this study are connected with (i) the use of highly textured samples, which were investigated in different orientations with respect to the γray direction, and (ii) the rigorous application of transmission-integral least-squares fit procedures. The latter enabled us to derive from the measured Mössbauer spectra reliable values for the relative amount of Fe^{2+} ions in the intercalant layers.

The magnetic properties of stage-2 $FeCl_3$-graphite are described by a spin-glass model, in agreement with previous suggestions.[3,14] The measurements in external magnetic fields reveal a strong in-plane coupling of the Fe^{3+} spins. It should also be mentioned that, in the temperature range from 2 to 4 K, less pronounced broadening effects due to magnetic relaxation are observed in the present work as compared to previous Mössbauer studies.[2,3] This hints at a better intercalant structure of the studied sample, which may be a consequence of the "soft" intercalation technique applied. The absence in our spectra of additional Fe^{3+} sites with a strong in-plane electric quadrupole interaction, which were reported in the work of Millman *et al.*[14] and which were attributed there to Fe vacancies, further supports this view.

The present Mössbauer results indicate that the Fe^{2+} ions are surrounded by Fe^{3+}. This would actually be in agreement with the formerly presented model of an Fe^{2+} superlattice.[9] On the other hand, such an Fe^{2+} superlattice needs an Fe^{2+} content of 25%, in clear disagreement

with the present result. Thus, the question of Fe^{2+} distribution, which is also relevant with respect to the magnetic interactions, remains open. Further experiments, like x-ray or neutron diffraction, as well as extended x-ray-absorption fine structure studies on highly textured samples should be most helpful in deciding on this question.

ACKNOWLEDGMENTS

This work was supported by the Sonderforschungsbereich 161 of the Deutsche Forschungsgemeinschaft, and by the Swiss National Science Foundation.

[1]M. S. Dresselhaus and G. Dresselhaus, Adv. Phys. **30**, 139 (1981).
[2]S. E. Millman, M. R. Corson, and G. R. Hoy, Phys. Rev. B **25**, 6595 (1982).
[3]D. Hohlwein, P. W. Readman, A. Camberod, and J. M. D. Coey, Phys. Status Solidi B **64**, 305 (1974).
[4]K. Ohhashi and I. Tsujikawa, J. Phys. Soc. Jpn. **36**, 442 (1974).
[5]R. Schlögl, P. Bowen, G. R. Millward, and W. Jones, J. Chem. Soc. Faraday Trans. **79**, 1793 (1983).
[6]R. Schlögl and W. Jones, Synth. Metals **7**, 133 (1983).
[7]G. K. Wertheim, P. M. van Attekum, H. J. Guggenheim, and K. E. Clements, Solid State Commun. **33**, 809 (1980).
[8]J. J. Ritsko and E. J. Mele, Physica **99B**, 425 (1980).
[9]S. E. Millman and G. Kirczenow, Solid State Commun. **44**, 1217 (1982).
[10]S. E. Millman and G. Kirczenow, Phys. Rev. B **28**, 5019 (1983).
[11]S. E. Millman, B. W. Holmes, and G. O. Zimmerman, Solid State Commun. **43**, 903 (1982).
[12]M. Elahy, C. Nicolini, G. Dresselhaus, and G. O. Zimmerman, Solid State Commun. **41**, 289 (1982).
[13]Ch. Simon, F. Batallan, I. Rosenman, J. Schweitzer, H. Lauter, and R. Vangelisti, Synth. Metals **8**, 53 (1983).
[14]S. E. Millman and G. O. Zimmerman, J. Phys. C **16**, L89 (1983).
[15]R. Schlögl and H. P. Boehm, Extended Abstract, Carbon '80, International Carbon Conference, Baden-Baden (1980) (unpublished), p. 114; see also Ref. 5.
[16]O. Beerkoz, M. Malamud, and S. Shtrikman, Solid State Commun. **6**, 185 (1968).
[17]R. H. Herber and H. Eckert, Phys. Rev. B **31**, 34 (1985).
[18]P. W. Anderson, J. Phys. Soc. Jpn. **9**, 93 (1954).
[19]A. Carrington and A. D. McLachlan, *Introduction to Magnetic Resonance* (Harper and Row, New York, 1969).
[20]G. K. Shenoy, J. M. Friedt, H. Maletta, and S. L. Ruby, Mössbauer Eff. Method. **9**, 277 (1974).
[21]H. Schäfer-Stahl, Synth. Metals **8**, 61 (1983).
[22]U. Gonser, *Mössbauer Spectroscopy* (Springer-Verlag, Berlin, 1975).
[23]L. E. Campbell, G. L. Montet, and G. J. Perlow, Phys. Rev. B **15**, 3318 (1977).
[24]J. M. Friedt, L. Soderholm, R. Perlow, and R. Vangelisti, Synth. Metals **8**, 99 (1983).
[25]G. Wortmann, I. Nowik, G. Kaindl, H. Selig, and I. Palchan, Synth. Metals **10**, 141 (1984).
[26]J. P. Stampfel, W. T. Oosterhuis, B. Window, and F. de S. Barros, Phys. Rev. B **8**, 4371 (1973).
[27]H. H. Wickman, M. P. Klein, and D. A. Shirley, Phys. Rev. **152**, 345 (1966).